

Reaction and structure effects of light mass nuclei using Glauber model with relativistic and non relativistic effective interaction densities

Mahesh K. Sharma¹, R. N. Panda², Manoj K. Sharma¹, and S. K. Patra³

¹*School of Physics and Materials Science, Thapar University, Patiala - 147 004, India.*

²*Department of Physics, ITER, Siksha O Anusandhan University, Bhubneswar-751 030, India and*

³*Institute of Physics, Sachivalaya marg Bhubneswar-751 005, India*

(Dated: August 28, 2018)

We study the structural properties of some nuclei in the region of light mass using simple effective interaction in the frame work of microscopic non relativistic Hartree-Fock and relativistic mean field formalisms. For the reaction dynamics, well known Glauber model is used with the conjunctions of the densities obtained from these formalisms. We observe good agreement of results by both the formalisms in comparison to the experimental values. These two different approaches seems to be equally capable to reproduce the ground state properties of nuclei in this region. A careful study of reaction dynamics suggest the superiority of relativistic mean field over the Hartree-Fock with simple effective interaction densities. But good agreement of reaction cross section is appeared with simple effective interaction density for halo nuclear systems. The possibility of existence of bubble nuclei are also studied using both the formalisms.

PACS numbers: 25.70.Jj, 25.60.Pj, 24.10-i, 25.70.-z, 27.90.+b

I. INTRODUCTION

The total reaction/interaction cross section measurements of nuclei at intermediate energy range has been extensively used to investigate the size of nucleus and distribution of nucleon in side the nucleus by the nuclear science community from more than one century [1–16]. The availability of heavy ion beams in intermediate energy range makes possible to explore the structures of nuclei over the wide range in nuclear chart. The advancement in radioactive ion beam facility (RIB) in this energy range at various laboratories over the globe open up new opportunities to investigate some new exotic phenomenon. The study of such exotic nuclei specially those towards the dripline and the investigation of extended dripline are some of the current interest [17–19]. Although earlier the dripline is well established for ^{24}O which is a doubly magic nuclei. The neutron separation energy and interaction measurement for $p - sd$ and sd shell region suggest the new magic number of $N=16$ [20] which is supported by Hoffman in Ref. [21]. The measurement of ^{40}Mg and ^{42}Al [22] beyond the dripline given by various mass formulae challenge the earlier predictions and still the investigation of dripline is a new challenge for both the nuclear theoretician and experimentalist. Apart from it the one most exotic phenomenon is the investigation of neutron and proton halo feature of some nuclei, which occurs due to the extremely weak bound neutrons that decouple from the nuclear core [10, 23]. Recently, a new member ^{31}Ne is included in the family of neutron halo [24, 25]. The isotope ^{31}Ne having $N=21$, breaks the shell closure structure and in consequence, a large amount of deformation gets associated with the strong intruder configuration and eventually this nuclear system lie at island of inversion (IOI) [26]. The investigation of nuclear systems at IOI is also be one of the current interest. The measurement of nuclear reaction cross-section

for $^{19,20,22}\text{C}$ [27, 28] shows that the drip-line nucleus ^{22}C has a halo. The one and two neutron removal cross sections and momentum distribution also support the halo behavior of ^{22}C . The ^{22}C has $N = 16$ which is a new magic number in neutron-rich nuclei [20, 29] and forms a Borromean halo structure (^{21}C is unstable). The direct time of flight mass measurement technique suggest ^{19}B , ^{22}C , ^{29}F and ^{34}Na are as Borromean dripline nuclei [30]. Another interesting phenomenon has been found in these days is the bubble structure of some nuclei like ^{22}O , ^{23}F , ^{34}Si , ^{36}S , ^{36}Ar , ^{46}Ar , ^{84}Se , ^{134}Ce , ^{174}Yb , ^{200}Hg etc. [31, 32]. The idea of bubble effect had been given by Wilson [33]. The possibility of formation of bubble nuclei has been studied by different nuclear models. The microscopic calculations using Skyrme Hartree-Fock (SHF) formalism have been carried for the investigation of this effect in Refs. [34–36]. Recently the relativistic and non relativistic mean field formalisms are used to investigate bubble effect in light [37] and superheavy region [38]. This effect also influence the reaction cross section of exotic nuclear systems.

The work done in Ref. [39] using the recently proposed simple effective interaction (SEI) in non relativistic mean field approach [40], successfully shows the good results of reaction cross sections for halo nuclear systems, which motivate us to see the reaction cross section for low mass region using this approach. For comparison, we used the well known relativistic mean field (RMF) densities using NL3 parameter set.

The paper is organized as, Section I consists of a brief introduction and Section II contains description of formalisms for relativistic and non relativistic mean field along with the Glauber model. The calculations and results are presented in Section III. The predictability of HF(SEI) model to explore the different features of nuclei are included in this section. Finally the summary and conclusions are outlined in Section IV.

II. THE FORMALISM

The bulk properties are very important for the study of the characteristics of nuclei. In this regards, well known relativistic mean field (RMF) and non relativistic mean field with newly developed simple effective interaction (SEI) are used. The well known Glauber approach is used here for the study of reaction dynamics for some light mass nuclei [41–43]. The study of reaction dynamics by this approach strongly depends on the densities of the projectile and target nuclei. We use densities from axially deformed (Def.) as well as spherically (Sph.) symmetric RMF formalisms. As we seen in our earlier calculation [44], the reaction cross section obtained from densities are parameters dependent upto some extent. So we used here, same set of parameter NL3 [45] in order to see the effect of deformations on reaction dynamics. The deformation effect is included in σ_R through densities of projectile and target nuclei by taking axially deformed RMF(NL3) densities. The same reaction study has been done by taking spherically symmetric densities from similar formalism for the sake of comparisons. We compare the results obtained from both relativistic mean field and non relativistic HF(SEI) densities. The simple effective interaction (SEI) with parametrization [40] are developed with non relativistic microscopic Hartree-Fock mean field theory. The detail about these formalisms and interaction parameters can be found in Refs. [45] and [40] for RMF and SEI, respectively. Here we used the densities from two different microscopic mean field formalisms to study their effect on the reaction dynamics.

A. Hartree-Fock with simple effective interactions

The simple effective interaction (SEI) alike to a hybrid of Gogny and Skyrme is used to study the bulk properties of finite nuclei with in the frame work of Hartree-Fock (HF) formalism. The form of simple effective interaction (SEI) is given by [40]

$$\begin{aligned} \nu_{eff}(r) = & t_0(1 + x_0 P_\sigma)\delta(r) \\ & + t_3(1 + x_3 P_\sigma)\left(\frac{\rho(R)}{1 + b\rho(R)}\right)^\gamma \delta(r) \\ & + (W + BP_\sigma - HP_\tau - MP_\sigma P_\tau)f(r), \end{aligned} \quad (1)$$

where, $f(r)$ is the functional form of the finite range interaction in term of Gaussian function $f(r) = e^{-r^2/\alpha^2}$ which contain a single range parameter α . The other terms having their usual meaning [40].

The Hamiltonian density functional using simple effective interaction is written as

$$\begin{aligned} \mathcal{H} = & \mathcal{K} + \mathcal{H}^{Nucl} + \mathcal{H}^{SO}(\mathbf{r}) \\ & + \mathcal{H}^{Coul}(\mathbf{r}) + \mathcal{H}^{RC}. \end{aligned} \quad (2)$$

Where $\mathcal{K} = \frac{\hbar^2}{2m}(\tau_n + \tau_p)$ is the kinetic energy term with τ_n and τ_p are the proton and neutron kinetic energy densities of nucleus. The second term of the Hamiltonian

is the nuclear contribution which contain the direct and exchange part. The direct contribution of nuclear energy density comes from the central part of the effective interaction. The third term is the spin-orbit interaction written as

$$\begin{aligned} \mathcal{H}^{SO}(\mathbf{r}) = & \frac{-1}{2}W_0[\rho(\mathbf{r})\nabla\mathbf{J} + \rho_n(\mathbf{r})\nabla\mathbf{J}_n \\ & + \rho_p(\mathbf{r})\nabla\mathbf{J}_p]. \end{aligned} \quad (3)$$

The fourth terms is due to Coulomb interaction which contains both direct and exchange terms given by

$$\mathcal{H}^{Coul}(\mathbf{r}) = \frac{1}{2} \int \frac{\rho_p(\mathbf{r}')}{|\mathbf{r} - \mathbf{r}'|} d^3r' - \frac{3}{4} \left(\frac{3}{\pi}\right)^{1/3} \rho_p^{4/3}. \quad (4)$$

The last term of the equation arises from the zero range part of the SEI, which plays the role of residual correlation energy.

$$\begin{aligned} \mathcal{H}^{RC} = & \frac{t_0}{4} \int [(1 - x_0)[\rho_n^2(\mathbf{r}) + \rho_p^2(\mathbf{r})]] \\ & + \frac{t_0}{4} \int [(4 + 2x_0)\rho_n(\mathbf{r})\rho_p(\mathbf{r})] \\ & + \frac{t_3}{24} \int [(1 - x_3)[\rho_n^2(\mathbf{r}) + \rho_p^2(\mathbf{r})]] \\ & + \frac{t_3}{24} \int [(4 + 2x_3)\rho_n(\mathbf{r})\rho_p(\mathbf{r})] \left(\frac{\rho(\mathbf{r})}{1 + b\rho(\mathbf{r})}\right)^\gamma. \end{aligned} \quad (5)$$

Here ρ_n , ρ_p , ρ , J_n , J_p and J are the neutron, proton and total nuclear and current densities respectively. The 12 parameters γ , b , t_0 , t_3 , x_0 , x_3 , W , B , H , M , α and W_0 are used for the calculation of ground state properties. The detailed procedure of calculations for ground state properties like binding energy, charge radius, nuclear matter radius etc. and parameters has been in Ref. [40].

B. Relativistic mean field Lagrangian density

The relativistic mean field formalism is well documented in Refs. [46–50]. The basic ingredient of RMF model is the relativistic Lagrangian density for a nucleon-meson many body system which is defined as [46–48]

$$\begin{aligned} \mathcal{L} = & \bar{\psi}_i(i\gamma^\mu\partial_\mu - M)\psi_i + \frac{1}{2}\partial^\mu\sigma\partial_\mu\sigma \\ & - \frac{1}{2}m_\sigma^2\sigma^2 - \frac{1}{3}g_2\sigma^3 - \frac{1}{4}g_3\sigma^4 - g_s\bar{\psi}_i\psi_i\sigma \\ & - \frac{1}{4}\Omega^{\mu\nu}\Omega_{\mu\nu} + \frac{1}{2}m_w^2V^\mu V_\mu \\ & - g_\omega\bar{\psi}_i\gamma^\mu\psi_iV_\mu - \frac{1}{4}\vec{B}^{\mu\nu}\cdot\vec{B}_{\mu\nu} \\ & + \frac{1}{2}m_\rho^2\vec{R}^\mu\cdot\vec{R}_\mu - g_\rho\bar{\psi}_i\gamma^\mu\vec{\tau}\psi_i\cdot\vec{R}_\mu \\ & - \frac{1}{4}F^{\mu\nu}F_{\mu\nu} - e\bar{\psi}_i\gamma^\mu\frac{(1 - \tau_{3i})}{2}\psi_iA_\mu. \end{aligned} \quad (6)$$

Here σ , V_μ and \vec{R}_μ are the fields for σ -, ω - and ρ -meson respectively. A^μ is the electromagnetic field. The ψ_i are the Dirac spinors for the nucleons whose third component of isospin is denoted by τ_{3i} . g_s , g_ω , g_ρ and $\frac{e^2}{4\pi} = \frac{1}{137}$ are the coupling constants for the linear term of σ -, ω - and ρ -mesons and photons respectively. g_2 and g_3 are the parameters for the non-linear terms of the σ -meson. M , m_σ , m_ω and m_ρ are the masses of the nucleons, σ -, ω - and ρ -mesons, respectively. $\Omega^{\mu\nu}$, $\vec{B}^{\mu\nu}$ and $F^{\mu\nu}$ are the field tensors for the V^μ , \vec{R}^μ and the photon fields, respectively. Now we used two assumptions, first the nucleons are moving inside the nucleus in spherically symmetric potential. In this case, the large and small component of Dirac spinor ψ_i are expanded separately in terms of radial function of a spherical harmonic oscillator potential and in second assumption, the nucleons are moving in non spherical symmetric potential. In this case the large and small component of Dirac spinor are expanded in axial symmetric manner in term of deformed harmonic oscillator potential by taking volume conservation into account. The set of Dirac and Klein-Gorden equation are solved by these two assumptions to obtain the bulk properties of nuclei. The quadrupole moment deformation parameter (β_2), root mean square radii (r_m) and binding energy (B.E.) are evaluated using the standard relations [48].

C. Glauber Model

1. (i) Reaction cross section

The theoretical formalism to study the reaction cross sections using the Glauber approach has been given by R. J. Glauber [5, 41]. The nucleus-nucleus elastic scattering amplitude is written as

$$F(q) = \frac{iK}{2\pi} \int db e^{iq \cdot b} (1 - e^{i\chi(b)}). \quad (7)$$

At low energy, this model is modified in order to take care of finite range effects in the profile function and Coulomb modified trajectories. The elastic scattering amplitude including the Coulomb interaction is expressed as

$$F(q) = e^{i\chi_s} \left\{ F_{coul}(q) + \frac{iK}{2\pi} \int db e^{iq \cdot b + 2i\eta \ln(Kb)} (1 - e^{i\chi(b)}) \right\}, \quad (8)$$

with the Coulomb elastic scattering amplitude

$$F_{coul}(q) = \frac{-2\eta K}{q^2} \exp\left\{-2i\eta \ln\left(\frac{q}{2K}\right) + 2i \arg \Gamma(1 + i\eta)\right\}, \quad (9)$$

where K is the momentum of projectile and q is the momentum transferred from the projectile to the target. Here $\eta = Z_P Z_T e^2 / \hbar v$ is the Sommerfeld parameter, v is the incident velocity of the projectile, and $\chi_s = -2\eta \ln(2Ka)$ with a being a screening radius. The elastic differential cross section is given by

$$\frac{d\sigma}{d\Omega} = |F(q)|^2. \quad (10)$$

The standard Glauber form for total reaction cross sections is expressed as [41, 42]

$$\sigma_R = 2\pi \int_0^\infty b [1 - T(b)] db, \quad (11)$$

where 'T(b)' is the Transparency function with impact parameter 'b'. The function T(b) is calculated by

$$T(b) = \exp\left[-\sum_{i,j} \sigma_{ij} \int \bar{\rho}_{tj}(s) \bar{\rho}_{pi}(|\vec{b} - \vec{s}|) d\vec{s}\right]. \quad (12)$$

Here, the summation indices i, j run over proton and neutron and subscript 'p' and 't' refers to projectile and target respectively. σ_{ij} is the experimental nucleon-nucleon reaction cross-section which depends on the energy. The z- integrated densities are defined as

$$\bar{\rho}(\omega) = \int_{-\infty}^\infty \rho(\sqrt{w^2 + z^2}) dz, \quad (13)$$

with $\omega^2 = x^2 + y^2$. Initially Glauber model was designed for the high energy approximation. However it was found to work reasonably well for both the nucleus-nucleus reaction and the differential elastic cross-sections over a broad energy range [43, 51]. The modified transparency function T(b) is given by

$$T(b) = \exp\left[-\int_p \int_t \sum_{i,j} [\Gamma_{ij}(\vec{b} - \vec{s} + \vec{t})] \bar{\rho}_{pi}(\vec{t}) \bar{\rho}_{tj}(\vec{s}) d\vec{s} d\vec{t}\right]. \quad (14)$$

The profile function Γ_{NN} for optical limit approximation is defined as

$$\Gamma_{NN} = \Gamma_{ij}(b_{eff}) = \frac{1 - i\alpha_{NN}}{2\pi\beta_{NN}^2} \sigma_{NN} \exp\left(-\frac{b_{eff}^2}{2\beta_{NN}^2}\right), \quad (15)$$

for finite range and

$$\Gamma_{NN} = \Gamma_{ij}(b_{eff}) = \frac{1 - i\alpha_{NN}}{2} \sigma_{NN} \delta(b), \quad (16)$$

for zero range with $b_{eff} = |\vec{b} - \vec{s} + \vec{t}|$, \vec{b} is the impact parameter. Where \vec{s} and \vec{t} are the dummy variables for integration over the z-integrated target and projectile densities. The parameters σ_{NN} , α_{NN} and β_{NN} are usually depends upon the proton-proton, neutron-neutron and proton-neutron interactions.

III. CALCULATIONS AND RESULTS

A. Ground state properties

The RMF(NL3) and HF(SEI) explain the nuclear properties like B.E. and rms radii reasonably well for almost all nuclei in the periodic chart. We use these sets to discuss the bulk properties of the considered nuclei.

TABLE I: The ground state properties of projectile and target nuclei obtained from RMF(NL3) and HF(SEI) calculations are compared with experimental data wherever available. The binding energy (B.E.) is in MeV and charge radius r_c is in fm.

Nuclei	B.E.				r_c			β_2		
	HF(SEI) (Sph.)	RMF(NL3) (Sph.)	RMF(NL3) (Def.)	Expt.[52, 53]	HF(SEI) (Sph.)	RMF(NL3) (Sph.)	RMF(NL3) (Def.)	Expt.[54]	RMF(NL3) (Def.)	Expt.[55]
⁹ Be	54.927	54.76	58.018	58.164±0.000	2.305	2.461	2.510	2.519	0.793	
¹⁰ Be	65.302	63.49	64.855	64.970±0.000	2.302	2.537	2.423	2.36	0.509	
¹¹ Be	69.380	67.97	67.780	65.478±0.000	2.329	2.479	2.449	2.46	0.369	
¹² Be	73.190	73.61	71.378	68.649±0.004	2.353	2.549	2.450		-0.137	
¹² B	82.172	82.85	82.176	79.575±0.001	2.393	2.498	2.457		0.168	
¹³ B	88.250	88.84	88.842	84.453±0.001	2.411	2.540	2.492		0.097	
¹⁴ B	89.256	91.88	89.874	85.423±0.021	2.423	2.534	2.522		0.382	
¹⁵ B	90.162	93.64	92.593	88.194±0.022	2.435	2.532	2.564	2.511	0.611	
¹² C	88.422	88.23	91.349	92.160±1.700	2.436	2.364	2.310	2.47	0.007	0.577(16)
¹³ C	97.489	96.31	98.098	97.108±0.000	2.454	2.459	2.466	2.46	-0.000	
¹⁴ C	105.829	104.38	106.929	105.284±0.000	2.470	2.504	2.517	2.56	0.000	0.36(3)
¹⁵ C	108.846	108.66	108.477	106.502±0.000	2.480	2.516	2.535		0.249	
¹⁶ C	111.642	113.45	111.874	110.752±0.003	2.489	2.531	2.565		0.448	
¹⁷ C	114.248	116.40	114.083	111.486±0.017	2.500	2.542	2.582		0.458	
¹⁸ C	116.709	118.79	116.842	115.670±0.030	2.509	2.552	2.601		0.471	
¹⁹ C	119.015	119.91	119.511	116.242±0.100	2.521	2.562	2.629		-0.438	
²⁰ C	121.154	122.54	119.736	119.18±0.200	2.532	2.573	2.590		0.278	
²⁰ N	139.487	139.37	136.772	134.184±0.055	2.605	2.671	2.683		-0.306	
²¹ N	143.095	142.59	141.475	138.768±0.100	2.614	2.674	2.694		-0.311	
²² N	146.205	145.55	143.948	140.052±0.200	2.624	2.679	2.678		-0.159	
²³ N	148.765	148.17	147.864	141.726±0.300	2.637	2.687	2.674		-0.009	
²⁰ O	154.043	152.71	151.585	151.36±0.100	2.668	2.720	2.726		0.250	0.268(6)
²¹ O	159.645	157.95	156.944	158.928±0.100	2.673	2.721	2.716		0.132	
²² O	164.758	164.18	163.192	166.496±0.100	2.678	2.735	2.712		0.002	0.19(4)
²³ O	169.040	168.32	167.227	174.064±0.100	2.689	2.741	2.725		0.003	
²⁴ O	172.508	171.87	171.665	181.632±0.100	2.701	2.752	2.737		0.003	
²³ F	177.956	176.75	175.378	175.283±0.100	2.768	2.839	2.805		-0.188	
²⁴ F	183.433	182.06	180.162	179.11±0.100	2.778	2.838	2.812		-0.128	
²⁵ F	186.026	186.90	185.221	183.375±0.100	2.782	2.853	2.821		-0.087	
²⁶ F	188.890	191.76	187.928	184.158±0.100	2.806	2.875	2.852		-0.125	
²⁷ F	191.507	195.00	191.245	186.246±0.200	2.827	2.891	2.886		0.151	
²⁸ Ne	207.273	210.62	208.122	206.89± 0.100	2.892	2.964	2.966	2.963	0.223	0.36(3)
²⁹ Ne	210.833	214.35	211.140	207.843±0.100	2.912	2.982	2.981		0.159	
³⁰ Ne	214.160	218.02	214.920	211.29±0.300	2.933	2.998	2.999		0.098	0.49(17)
³¹ Ne	214.569	221.97	215.812	211.42±0.200	2.944	3.012	3.032		0.238	
³² Ne	214.860	223.95	218.409	213.472±0.500	2.956	3.024	3.071		0.363	
³² Mg	249.390	252.06	250.387	249.804±0.200	3.032	3.095	3.091	3.186	0.119	0.51(5)
³³ Mg	252.015	256.02	252.982	252.017±0.200	3.043	3.107	3.118		0.231	
³⁴ Mg	254.355	259.14	257.169	256.462±0.100	3.053	3.118	3.151		0.340	0.55(6)
³⁵ Mg	256.498	261.82	260.211	257.460±0.200	3.064	3.129	3.174		0.385	
³² Si	267.928	267.69	268.203	271.407±0.000	3.078	3.113	3.141		-0.203	0.26(4)
³³ Si	275.953	275.97	275.359	275.915±0.000	3.095	3.133	3.134		-0.085	
³⁴ Si	283.470	283.78	278.249	283.428±0.014	3.111	3.153	3.206		-0.337	0.18(4)
³⁵ Si	288.258	289.77	287.135	285.903±0.038	3.119	3.163	3.164		-0.084	
³⁴ S	286.424	286.05	286.295	291.838±0.000	3.199	3.270	3.259	3.28	-0.168	0.247(3)
³⁵ S	296.491	296.71	295.543	298.824±0.000	3.209	3.282	3.262		-0.077	
³⁶ S	305.978	306.52	299.502	308.714±0.000	3.219	3.293	3.312	3.29	-0.309	0.157(7)
³⁷ S	312.676	313.58	309.946	313.017±0.000	3.224	3.299	3.290		-0.116	
³⁴ Ar	273.357	273.76	273.397	278.719±0.000	3.295	3.387	3.360	3.365	-0.168	0.229(15)
³⁶ Ar	300.129	300.25	302.268	306.716±0.000	3.305	3.388	3.379	3.390	-0.209	0.253(8)
³⁸ Ar	324.432	325.59	319.946	327.342±0.000	3.318	3.397	3.396	3.402	-0.279	0.161(4)
⁴⁰ Ar	341.555	342.31	340.945	343.810±0.000	3.326	3.401	3.392	3.427	-0.160	0.269(5)
⁴² Ar	357.013	357.39	356.393	359.335±0.005	3.335	3.406	3.402	3.435	-0.176	0.27(3)
⁴⁴ Ar	371.135	371.42	370.639	373.728±0.001	3.345	3.410	3.410	3.445	-0.179	0.22(16)
⁴⁶ Ar	383.672	384.57	384.603	386.927±0.040	3.373	3.410	3.415	3.437	-0.167	0.170(17)
⁴⁸ Ar	391.79	394.58	392.810	396±0.720	3.393	3.437	3.442		-0.198	

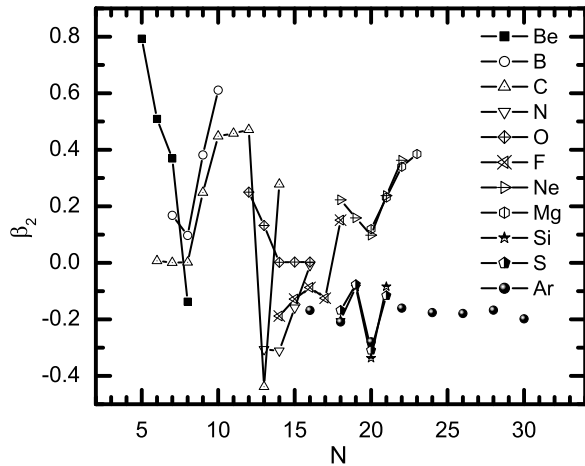


FIG. 1: The quadrupole deformation parameter β_2 of ^{9-12}Be , $^{12-15}\text{B}$, $^{12-20}\text{C}$, $^{20-23}\text{N}$, $^{20-24}\text{O}$, $^{23-27}\text{F}$, $^{28-32}\text{Ne}$, $^{32-35}\text{Mg}$, $^{32-35}\text{Si}$, $^{34-37}\text{S}$ and $^{34-48}\text{Ar}$ as a function of neutron number (N) for RMF(NL3).

1. Binding energy

The binding energies (B.E.'s) of ^{9-12}Be , $^{12-15}\text{B}$, $^{12-20}\text{C}$, $^{20-23}\text{N}$, $^{20-24}\text{O}$, $^{23-27}\text{F}$, $^{28-32}\text{Ne}$, $^{32-35}\text{Mg}$, $^{32-35}\text{Si}$, $^{34-37}\text{S}$ and $^{34-48}\text{Ar}$ obtained by relativistic mean field theory using spherical and axially deformed coordinates systems and with non relativistic mean field theory using simple effective interaction are presented in Table I along with experimental values. The B.E. of ^{10}Be are 65.302, 63.49 and 64.855 MeV for HF(SEI), Sph. RMF(NL3) and Def. RMF(NL3) formalisms, well comparable to its experimental value 64.970 MeV. Hence by examining the results of Table I, it can be concluded that both the formalisms are capable to reproduce the experimental data for the considered nuclei.

2. Charge radius

The calculated root mean square charge radius (r_c) of projectile and target nuclei from both RMF(NL3) and non relativistic HF(SEI-I) mean field theories are presented in Table I. The experimental data are also given for comparison wherever available [54]. The rms proton radius r_p is obtained from the distribution of point protons inside the nucleus. The charge radius r_c is calculated by taking the finite size 0.8 fm of the proton, which is evaluated from the formula $r_c = \sqrt{r_p^2 + 0.06}$ [48]. The calculated values of r_c for ^{11}Be are 2.329, 2.479 and 2.449 fm from HF (SEI), Sph. RMF(NL3) and Def. RMF(NL3) formalisms, which are well comparable with the experimental value of 2.46 fm. Similarly r_c for ^{36}Ar and ^{46}Ar are 3.035 fm, 3.373 fm for HF(SEI), 3.388 fm,

3.410 fm for Sph. RMF(NL3), 3.379 fm, 3.415 fm for Def. RMF(NL3) and 3.390 fm, 3.437 fm for experimental observations, respectively. In general, observation from this table signifies the successability of these theories by predicting the surprisingly comparable results with experimental data.

3. Quadrupole deformation parameter β_2

Figure 1 shows the quadrupole deformation parameter (β_2) of considered cases of nuclei obtained from RMF(NL3) formalism as a function of their neutron numbers of the isotopes. Table I also presents the values of deformation along with the experimental values which are available. The negative β_2 values of nuclei in Table I signifies its oblate deformation where as positive values of prolate deformation and zero value of spherical nature. It is worthy to mention that the NL3 parameter set does not give a converged solution for many of the light nuclei as such. To get a converged result for such cases, we change the pairing strength $\Delta_{n,p}$ slightly in the BCS-pairing approach. As a result, we compromise a bit in the quadrupole deformation.

4. Density

Fig. 2 presents the densities of the considered nuclei as a function of radial distance (r in fm). The nucleons distribution inside the nucleus is maximum at the centre and starts decreasing continuously towards the surface. The left panel of the figure presents the nucleonic density distribution obtained by non relativistic mean field HF(SEI) approach. The right panel shows spherical equivalent of deformed RMF densities with NL3 parameter. The central panel of the figure shows the density distribution obtained from spherical symmetric RMF model. It is clear from the figure that the densities of considered nuclei shows similar kind of trend from all the formalisms. A deep inspection of the figure indicates some of the isotopes of O, F, Si, S and Ar shows depletion of the densities at the centre, which is the primary indication for their bubble structure.

Some of the prominent cases of bubble nuclei are plotted in Fig. 3. This figure contains the proton and neutron density distributions of ^{22}O , ^{23}F , ^{34}Si , ^{36}S , ^{36}Ar and ^{46}Ar nuclei as a function of radial distance. The left panel of the figure shows the neutron and right panel shows proton density distribution of considered cases of nuclei for HF(SEI), Sph. RMF(NL3) and Def. RMF(NL3) densities, respectively. It is clear from the figure, the depletion for proton density distribution is more than the neutron counterpart. Detailed discussion of bubble nuclei has been given in next subsection.

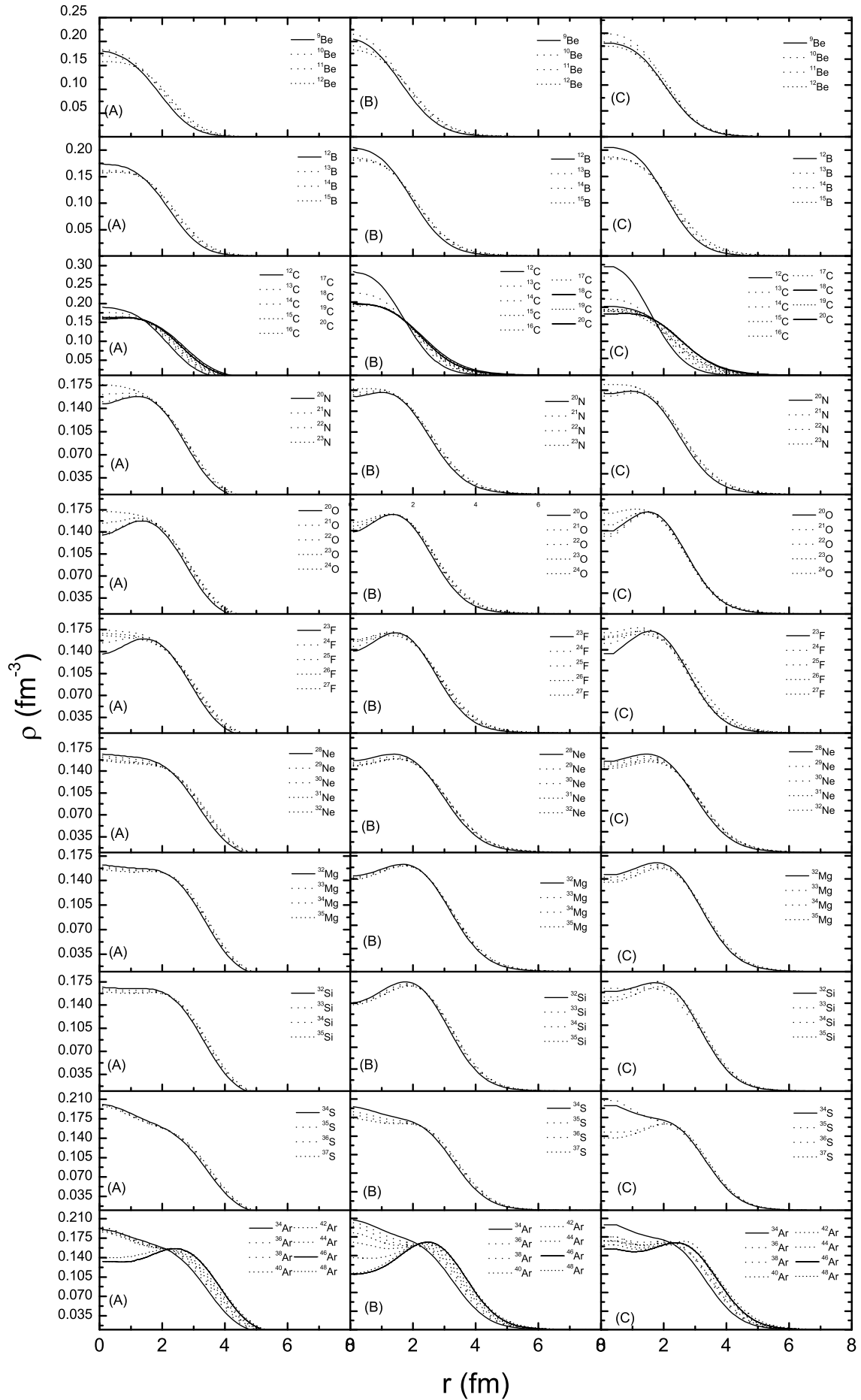


TABLE II: The Depletion Factor (D.F in %) of neutron (N), proton (P) and total (T) densities for some probable cases of bubble nuclei obtained from HF(SEI), Sph. RMF(NL3) and Def. RMF(NL3).

Nuclei	D.F.%			D.F.%			D.F.%		
	HF(SEI)			Sph. RMF			Def. RMF		
	N	P	T	N	P	T	N	P	T
^{22}O	8.21	19.14	13.21	9.49	20.23	14.46	24.35	22.47	23.29
^{23}F	10.67	20.45	15	14.44	22.71	18.26	22.14	22.30	21.99
^{34}Si	-	36.66	-	0.36	36.27	16.75	-	3.73	-
^{36}S	-	-	-	-	-	-	3.49	16.25	9.49
^{36}Ar	-	-	-	-	-	-	-	-	-
^{46}Ar	-	51.05	14.74	15.31	62.08	36.64	1.56	14.73	7.51

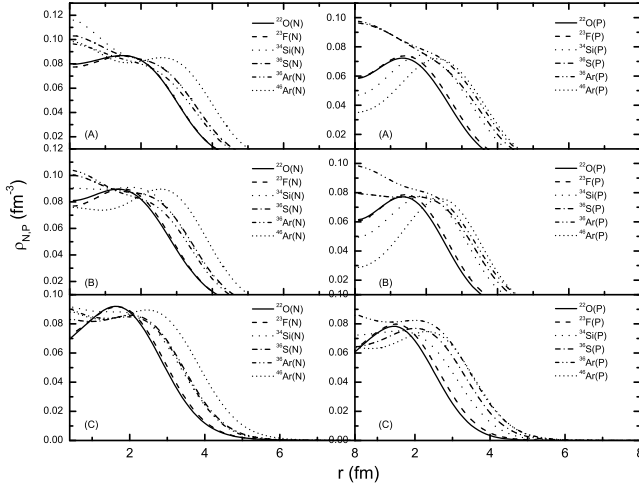


FIG. 3: Radial density plots for expected bubble nuclei ^{22}O , ^{23}F , ^{34}Si , ^{36}S , ^{36}Ar and ^{46}Ar obtained by (A) HF(SEI) (B) Sph. RMF(NL3) (C) Def. RMF(NL3) formalisms.

B. Bubble nuclei

The bubble effect is appeared in some of the nuclei, where the density of nucleus is depleted at central part. The main mechanism for the formation of bubble nuclei is the lack of particles in the centre of nucleus which causes the s levels to be less bound than observed in the usual cases with the uniform density distribution. If the particles rise high enough in energy, highest s levels will be empty, hence depletion of central density of particles takes place as a consequence, the radius of the nucleus increases. The depleted density of nuclei has been measured in term of depletion factor (D. F.) defined as [31]

$$D.F. = \frac{\rho_{max} - \rho_{cen}}{\rho_{max}}, \quad (17)$$

where ρ_{max} and ρ_{cen} represent the values of maximum and the central density. The calculated values of D. F. in % for the ^{22}O , ^{23}F , ^{34}Si , ^{36}S , ^{36}Ar and ^{46}Ar are presented

in Table II. The value of $(D.F.)_T$ in % for ^{22}O are 13.21%, 14.46% and 23.28% for the HF(SEI), Sph. RMF(NL3) and Def. RMF(NL3) densities. Similarly the $(D.F.)_T$ for the ^{23}F are 15%, 18.26% and 21.99% from same densities, respectively. The $(D.F.)_P$ in % for the ^{34}Si and ^{46}Ar nuclei are 36.36% and 51.06% for HF(SEI), 36.27% and 62.08% for Sph. RMF(NL3) and 3.72% and 14.72% for Def. RMF(NL3) densities indicate the nature of their proton bubble. The observations from this table also signifies, no bubble effect for ^{36}Ar and 16.25% $(D.F.)_P$ for ^{36}S in Def. RMF(NL3) case indicates, it may be a case for proton bubble along with ^{34}Si and ^{46}Ar nuclei. Thus prominent cases for bubble effects are found in ^{22}O , ^{23}F , ^{34}Si and ^{46}Ar from our study.

C. Total reaction cross section

The main ingredient of the Glauber model is the densities of projectile and target nuclei. The densities from the well known RMF with NL3 parameter are used from both axially deformed and spherically symmetric formalisms along with the densities of HF(SEI-I). As our earlier work increase curiosity to see the effect of simple effective interaction on reaction dynamics. We need these densities in terms of the Gaussian coefficients for the investigation of reaction dynamics. We converted these densities of HF(SEI), Sph. RMF(NL3) as well as Def. RMF(NL3) in term of Gaussian coefficients as

$$\rho(r) = \sum_{i=1}^2 c_i \exp[-a_i r^2]. \quad (18)$$

TABLE III presents spherical and deformed densities from RMF(NL3) along with non relativistic HF(SEI-I) densities in terms of their Gaussian coefficients c_i and a_i . Another important ingredient for evaluation of profile function in Glauber model is energy dependent parameters σ_{NN} , α_{NN} and β_{NN} , where σ_{NN} is the total nuclear reaction cross section in NN collision, α_{NN} is ratio of real to the imaginary part of forward nucleon-nucleon scattering amplitude and β_{NN} is slope parameter, which determines the fall of the angular distribution of the NN scattering. These parameters are energy as well isospin

TABLE III: The Gaussian coefficients c_1 , a_1 , c_2 , a_2 of projectile and target for HF(SEI), Sph. RMF(NL3) and Def. RMF(NL3) densities.

<i>Nuclei</i>	HF(SEI-I)				Sph. RMF(NL3)				Def. RMF(NL3)			
	c_1	a_1	c_2	a_2	c_1	a_1	c_2	a_2	c_1	a_1	c_2	a_2
⁹ Be	-2.51177	0.393812	2.69169	0.37377	-0.0593744	0.659468	0.268817	0.289419	-1.25421	0.39907	1.39728	0.355553
¹⁰ Be	-3.33309	0.379659	3.51516	0.363426	-0.0915913	0.609445	0.312021	0.291001	-1.22148	0.413105	1.39161	0.361781
¹¹ Be	-3.04829	0.355441	3.2177	0.338208	-0.122702	0.527202	0.319249	0.268455	-1.21881	0.390577	1.38332	0.340326
¹² Be	-1.35748	0.35003	1.51497	0.311617	-0.311776	0.455307	0.521176	0.300176	-0.995759	0.218859	1.20496	0.217494
¹² B	-3.63908	0.350342	3.80913	0.334343	-1.50466	0.407157	1.70762	0.358788	-1.19869	0.404408	1.39307	0.347786
¹³ B	-3.94932	0.335534	4.10771	0.320364	-2.67497	0.375355	2.85669	0.347163	-0.499802	0.428431	0.677544	0.30021
¹⁴ B	-3.93077	0.321021	4.08801	0.306225	-0.86619	0.390135	1.04795	0.310126	-0.210262	0.478779	0.376203	0.242406
¹⁵ B	-1.60867	0.317723	1.76563	0.283852	-0.466283	0.412755	0.645633	0.276104	-1.07423	0.297112	1.23432	0.259716
¹² C	-3.79616	0.361674	3.98071	0.345423	-0.232654	0.638687	0.0517232	0.339911	-1.14333	0.285974	1.47032	0.285598
¹³ C	-1.74891	0.355312	1.9196	0.320299	-1.44407	0.413914	1.64276	0.355309	-1.17196	0.403733	1.40401	0.345876
¹⁴ C	-1.88677	0.342428	2.04598	0.308693	-3.77882	0.365346	3.96791	0.344481	-1.18651	0.385936	1.37994	0.324587
¹⁵ C	-1.90963	0.327595	2.0674	0.295423	-4.16046	0.35900	4.33524	0.338276	-0.294377	0.45885	0.472115	0.256238
¹⁶ C	-1.9147	0.314974	2.07175	0.283792	-1.6802	0.35973	1.85217	0.311381	-1.21984	0.316502	1.38936	0.27335
¹⁷ C	-1.91276	0.303614	2.06889	0.273238	-3.52531	0.332303	3.69421	0.3095	-1.15816	0.309391	1.32105	0.263253
¹⁸ C	-1.93748	0.292373	2.0941	0.263313	-0.22627	0.429346	0.432019	0.225458	-1.19721	0.300572	1.35334	0.255236
¹⁹ C	-1.94062	0.280481	2.09825	0.25306	-2.6298	0.312787	2.79198	0.284036	-0.61523	0.331571	0.866337	0.257346
²⁰ C	-4.27647	0.261466	4.43707	0.24962	-2.58028	0.302332	2.73839	0.273816	-0.162047	0.423205	0.350278	0.191529
²⁰ N	-2.27523	0.279519	2.41666	0.253036	-1.65348	0.298831	1.82293	0.260481	-0.760729	0.309713	0.966724	0.24428
²¹ N	-2.28047	0.269391	2.42488	0.244319	-1.28808	0.292176	1.46044	0.246603	-0.795721	0.306924	0.998833	0.240861
²² N	-2.16896	0.25557	2.32419	0.232462	-1.21886	0.280349	1.39582	0.236182	-1.16072	0.24254	1.36471	0.215256
²³ N	-4.08043	0.234574	4.25039	0.224176	-1.21542	0.266098	1.39836	0.226368	-0.329494	0.133146	0.523324	0.132026
²⁰ O	-2.47486	0.286301	2.60404	0.25909	-5.45193	0.299258	5.58882	0.284173	-1.93556	0.310064	2.05253	0.267917
²¹ O	-2.53565	0.27829	2.66435	0.252158	-2.00566	0.303822	2.14271	0.264553	-1.51258	0.315625	1.63101	0.260035
²² O	-2.57536	0.269317	2.7064	0.244573	-1.86978	0.293242	2.01341	0.254045	-0.64512	0.363379	0.764856	0.230878
²³ O	-2.43928	0.254471	2.58493	0.232008	-1.80269	0.282707	1.9515	0.244704	-0.657758	0.330368	0.802805	0.223554
²⁴ O	-2.04609	0.239581	2.20933	0.217663	-1.92109	0.267916	2.07684	0.235596	-0.668732	0.297564	0.838554	0.214713
²³ F	-2.69853	0.263769	2.82652	0.23994	-5.77017	0.27426	5.90555	0.260946	-2.48442	0.288719	2.59277	0.254931
²⁴ F	-2.42788	0.249261	2.57181	0.226755	-2.13084	0.274675	2.27389	0.241917	-0.885032	0.274091	1.06166	0.217354
²⁵ F	-2.09825	0.2342	2.26064	0.212972	-1.99848	0.261501	2.15224	0.230625	-0.763297	0.238881	0.956929	0.196001
²⁶ F	-2.06675	0.224826	2.22373	0.20445	-1.94522	0.249237	2.09993	0.220358	-0.742259	0.240026	0.928872	0.19271
²⁷ F	-2.03263	0.216267	2.18559	0.196679	-1.94413	0.238163	2.09571	0.211318	-1.85421	0.23814	1.99459	0.209488
²⁸ Ne	-2.10042	0.212881	2.2517	0.19371	-2.17488	0.232385	2.32326	0.208284	-0.937098	0.256729	1.11394	0.202448
²⁹ Ne	-2.07765	0.205597	2.22506	0.187105	-2.31443	0.224436	2.45925	0.202571	-0.919743	0.232073	1.09489	0.187997
³⁰ Ne	-2.05061	0.198501	2.19404	0.180662	-2.34129	0.215415	2.48218	0.195104	-0.815071	0.213394	0.985336	0.173332
³¹ Ne	-2.07274	0.194286	2.2139	0.176848	-2.30031	0.214514	2.44391	0.193464	-0.896996	0.216244	1.0655	0.17556
³² Ne	-4.57748	0.184948	4.71668	0.177083	-2.26169	0.211097	2.40614	0.189954	-0.928504	0.2197	1.09451	0.176494
³² Mg	-2.20212	0.194812	2.34336	0.177429	-2.60897	0.212996	2.74249	0.193239	-0.967166	0.213458	1.13137	0.174275
³³ Mg	-2.22698	0.191053	2.36594	0.174019	-2.60291	0.209569	2.73607	0.18993	-1.07939	0.221034	1.24224	0.179671
³⁴ Mg	-2.24103	0.18709	2.37778	0.170425	-2.58898	0.206733	2.72212	0.187059	-1.06206	0.23098	1.22155	0.182458
³⁵ Mg	-2.26351	0.183622	2.39807	0.167282	-2.5666	0.203774	2.69959	0.184066	-1.05435	0.230207	1.21082	0.180174
³² Si	-2.37277	0.202381	2.51805	0.184376	-3.00897	0.227291	3.13661	0.206144	-0.975703	0.260388	1.13915	0.19639
³³ Si	-2.35386	0.196639	2.49616	0.179151	-2.9272	0.218848	3.05298	0.198521	-0.995642	0.223719	1.1529	0.178138
³⁴ Si	-2.34203	0.191388	2.48123	0.174374	-2.86769	0.211811	2.99191	0.192149	-1.25717	0.26293	1.42724	0.204504
³⁵ Si	-2.36933	0.187986	2.50617	0.171288	-2.88628	0.208281	3.00941	0.188926	-1.09127	0.208147	1.24501	0.169924
³⁴ S	-1.81296	0.181829	1.98726	0.165612	-2.03669	0.193789	2.20712	0.175664	-1.18862	0.215201	1.38091	0.180478
³⁵ S	-1.78947	0.176802	1.96139	0.161028	-2.11099	0.189798	2.27085	0.172077	-1.18643	0.175455	1.38282	0.156079
³⁶ S	-1.76837	0.172069	1.93796	0.156714	-2.13714	0.185085	2.28947	0.167819	-1.52688	0.248852	1.67126	0.199451
³⁷ S	-1.79518	0.169348	1.96303	0.154256	-2.21565	0.183299	2.3634	0.166219	-1.07227	0.2135	1.21247	0.168601
³⁴ Ar	-1.93044	0.183573	2.09551	0.167211	-1.84812	0.18999	2.02988	0.172144	-1.18677	0.213069	1.38036	0.179369
³⁶ Ar	-1.83132	0.172884	1.99595	0.157479	-1.79242	0.177609	1.96319	0.160928	-1.25018	0.223959	1.41575	0.181827
³⁸ Ar	-1.79848	0.164912	1.96024	0.150194	-1.82537	0.169399	1.98489	0.153507	-1.76793	0.225418	1.92718	0.189616
⁴⁰ Ar	-1.85865	0.160185	2.01657	0.145936	-1.99749	0.166945	2.14665	0.151332	-1.18469	0.194597	1.34956	0.160534
⁴² Ar	-1.91109	0.155909	2.06565	0.142049	-2.26358	0.166337	2.39771	0.150869	-1.18071	0.197867	1.33743	0.1597
⁴⁴ Ar	-1.96876	0.151999	2.11994	0.138517	-2.68801	0.168372	2.79633	0.152825	-1.18782	0.195138	1.33648	0.156048
⁴⁶ Ar	-2.01107	0.148333	2.17100	0.134800	-2.71107	0.167337	2.83113	0.151854	-1.18885	0.194037	1.33033	0.154800

TABLE IV: The nucleon-nucleon cross-section σ_{NN} and other parameters like α_{NN} and β_{NN} used to calculate the profile function.

$E(\text{MeV}/A)$	$\sigma_{NN} (fm^2)$	α_{NN}	$\beta_{NN}(fm^2)$
230.0	3.307790	0.7462136	0.1042526
240.0	3.266868	0.6800303	0.0978437
730.0	4.174130	-0.0828693	0.1896611
740.0	4.189708	-0.0793203	0.1931483
760.0	4.217336	-0.0731153	0.1996571
790.0	4.250772	-0.0691061	0.2078210
900.0	4.311690	-0.1439280	0.2171934
905.0	4.312775	-0.1498595	0.2170294
920.0	4.315433	-0.1684008	0.2163436
950.0	4.318554	-0.2078482	0.2142974
955.0	4.318853	-0.2146004	0.2138945
960.0	4.319103	-0.2213738	0.2134798
965.0	4.319310	-0.2281574	0.2130555
980.0	4.319725	-0.2484590	0.2117466
1005.0	4.320055	-0.2814692	0.2095773
1010.0	4.320110	-0.2878605	0.2091625
1020.0	4.320220	-0.3004108	0.2083566

dependent. Table IV contains these energy dependent parameters over energy range (230-1020)MeV/A. These parameters have been estimated by using the spline interpolation of values as suggested in Ref. [56].

The calculated values of reaction cross sections for considered nuclei using the HF(SEI), Sph. RMF(NL3) and Def. RMF(NL3) densities are presented in the TABLE V. The calculated values of reaction cross sections are also compared with the experimental data. It seen from the TABLE, the σ_R obtained from both relativistic and non-relativistic formalisms are well comparable with the experimental observation. To analysis of the observation we used the χ^2 fitting. The chi-square fitting (χ^2 -fitting) can be defined as

$$\chi^2 = \sum \chi_i^2 = \sum_i \frac{(\sigma_R(Obs) - \sigma_R(Exp))^2}{\sigma_R(Exp)}. \quad (19)$$

The table also presents the χ_i^2 fitting values of σ_R for various densities with experimental observations. The overall χ^2 fitting values for HF(SEI), spherical RMF(NL3) and Deformed RMF(NL3) densities are 753.157, 189.335 and 493.407 respectively. The values of σ_R for the ^{11}Be , ^{15}C , ^{19}C , ^{23}O and ^{31}Ne halo nuclei are 942, 1065, 1215, 1327, 1481 in mb for HF(SEI), 902, 1026, 1120, 1257, 1408 in mb for Def. RMF(NL3), 890, 959, 1099, 1218, 1353 in mb for Sph. RMF(NL3) densities and 942 ± 8 , 945 ± 10 , 1231 ± 28 , 1308 ± 16 , 1435 ± 22 in mb from the experimental data. The value of χ^2 is small for the Sph. RMF(NL3) density shows, the σ_R obtained with this density reproduced better results as compare to the other cases.

By looking deep into the table one can easily interpret

that the values of reaction cross sections obtained for particular halo systems and other exotic nuclei shows better results with deformed RMF(NL3) and HF(SEI) densities.

Fig. 4 shows the total reaction cross sections of ^{9-12}Be , $^{12-15}\text{B}$, $^{13-20}\text{C}$, $^{20-23}\text{N}$, $^{20-24}\text{O}$, $^{23-27}\text{F}$, $^{28-32}\text{Ne}$, $^{32-35}\text{Mg}$, $^{32-35}\text{Si}$, $^{34-37}\text{S}$ and $^{34-48}\text{Ar}$ nuclei as a function of projectile energy (E_{proj}) over the energy range of (30-1000) MeV/Nucleon. The value of σ_R has higher value at small E_{proj} and start decreasing upto the energy range of 300 MeV/nucleon. Small enhancement in σ_R is observed upto the range of 750 MeV/nucleon and after that, it remains constant. The observation from the table shows the values of σ_R obtained from the HF(SEI) densities are slightly higher than the other densities. The value of σ_R also increases by equal proportion in their isotopic chain as a mass number for both cases of HF(SEI) and Sph. RMF(NL3) densities. But some disorder in increase of the σ_R is appeared for the case Def. RMF(NL3) densities. This effect may be because of the role of deformation in σ_R .

IV. SUMMARY AND CONCLUSIONS

In summary, we study the structural properties and σ_R for ^{9-12}Be , $^{12-15}\text{B}$, $^{13-20}\text{C}$, $^{20-23}\text{N}$, $^{20-24}\text{O}$, $^{23-27}\text{F}$, $^{28-32}\text{Ne}$, $^{32-35}\text{Mg}$, $^{32-35}\text{Si}$, $^{34-37}\text{S}$ and $^{34-48}\text{Ar}$ nuclei using the densities from the non relativistic Hartree-Fock with simple effective interaction as well as relativistic mean field formalism. The bulk properties like binding energy, charge radius and quadrupole deformation parameter β_2 are studied with these formalisms which shows good agreement with the experimental data. Bubble effects for some of the nuclei like ^{22}O , ^{23}F , ^{34}Si and ^{46}Ar are appeared by our study. Such effects are required on nuclear structure and reaction studies in dripline as well as superheavy region. The σ_R obtained with the RMF formalism shows better results as compare to the non relativistic HF(SEI) densities for general cases. But the remarkable agreement is appeared with HF(SEI) densities for the halo nuclear systems as compare to RMF densities. In general, we found both the formalisms are equally capable for the study of structure and reaction dynamics for most of the nuclear systems in the light mass region. It needs further investigations to see effect of these formalisms on other nuclear systems in both medium and heavy mass regions.

Acknowledgments

One of the author Mahesh K. Sharma thanks the institute of Physics, Bhubaneswar for their kind hospitality.

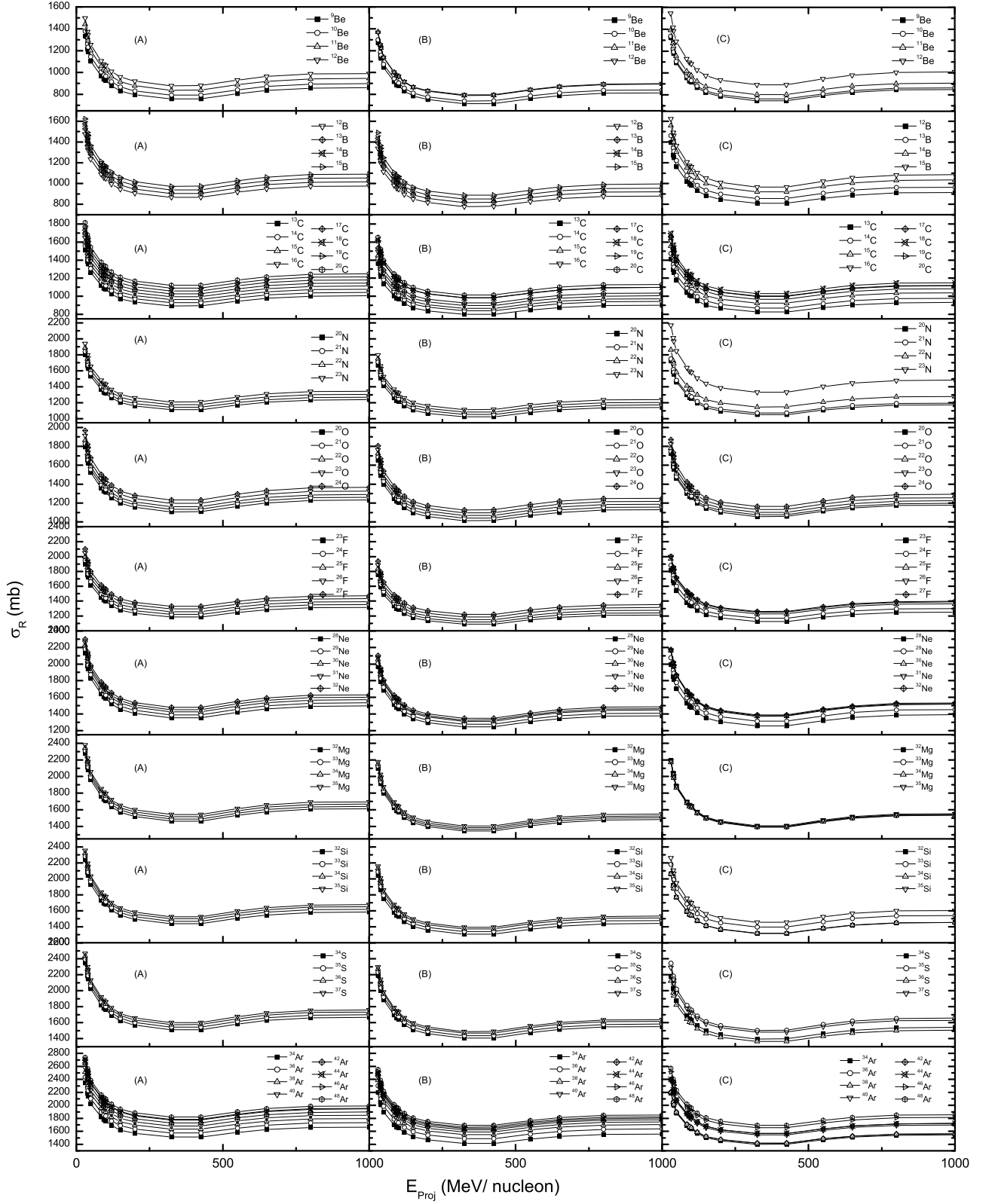


FIG. 4: Variation of total reaction cross sections (σ_R) as a projectile energy (E_{proj}) using (A) HF(SEI), (B) Sph. RMF(NL3), (C) Def. RMF(NL3) densities for isotopes of $^9\text{--}^{12}\text{Be}$, $^{12\text{--}15}\text{B}$, $^{13\text{--}20}\text{C}$, $^{20\text{--}23}\text{N}$, $^{20\text{--}24}\text{O}$, $^{23\text{--}27}\text{F}$, $^{28\text{--}32}\text{Ne}$, $^{32\text{--}35}\text{Mg}$, $^{32\text{--}35}\text{Si}$, $^{34\text{--}37}\text{S}$ and $^{34\text{--}48}\text{Ar}$ nuclei.

TABLE V: Total nuclear reaction cross section with various projectiles with ^{12}C target. The experimental data [57] are given for comparison.

Proj.	Energy (A MeV)	$\sigma_R(mb)$			Expt.	χ^2		
		HF(SEI-I) (sph.)	RMF(NL3) (sph.)	RMF(NL3) (Def.)		HF(SEI-I) (Sph.)	RMF(NL3) (Sph.)	RMF(NL3) (Def.)
^9Be	790	857	810	844	806±9	3.227	0.020	5.907
^{10}Be	790	894	836	860	813±10	8.070	0.651	6.027
^{11}Be	790	942	890	902	942±8	0.000	2.870	0.000
^{12}Be	790	986	894	1004	927±18	3.755	1.175	1.247
^{12}B	790	972	875	909	866±7	12.975	0.094	3.621
^{13}B	790	1012	916	960	883±14	18.846	1.233	7.248
^{14}B	790	1049	951	1029	929±26	15.501	0.521	10.338
^{15}B	790	1086	991	1080	962±160	15.983	0.874	21.856
^{13}C	960	1005	901	931	862±12	23.723	1.765	5.208
^{14}C	965	1003	944	978	880±19	17.192	4.655	10.473
^{15}C	730	1065	959	1026	945±10	15.238	0.207	5.795
^{16}C	960	1113	1005	1084	1036±11	5.723	0.928	3.831
^{17}C	965	1147	1037	1117	1056±10	7.842	0.342	5.910
^{18}C	955	1182	1098	1150	1104±15	5.511	0.033	4.066
^{19}C	960	1215	1099	1120	1231±28	0.208	14.154	0.007
^{20}C	905	1271	1131	1179	1187±20	5.944	2.642	3.033
^{20}N	950	1239	1141	1174	1121±17	12.421	0.357	1.031
^{21}N	1005	1270	1172	1195	1114±9	21.846	3.020	13.581
^{22}N	965	1306	1205	1278	1245±49	2.989	1.285	0.001
^{23}N	920	1344	1240	1483	1399±98	2.162	18.071	8.807
^{20}O	950	1233	1130	1179	1078±10	22.287	2.508	7.348
^{21}O	980	1261	1158	1197	1098±11	24.198	3.279	8.219
^{22}O	965	1291	1188	1225	1172±22	12.083	0.218	2.049
^{23}O	960	1327	1218	1257	1308±16	0.276	6.193	2.398
^{24}O	965	1367	1251	1292	1318±52	1.822	3.406	0.777
^{23}F	1020	1316	1211	1250	1148±16	24.585	3.457	8.537
^{24}F	1005	1354	1242	1299	1253±23	8.141	0.097	0.352
^{25}F	1010	1393	1276	1363	1298±31	6.953	0.373	0.093
^{26}F	950	1434	1315	1388	1353±54	4.849	1.067	0.018
^{28}Ne	240	1382	1272	1283	1273±11	9.333	0.001	4.186
^{29}Ne	240	1417	1302	1340	1344±14	3.965	1.313	0.003
^{28}Ne	950	1497	1378	1391	1244±40	51.454	14.434	36.814
^{29}Ne	950	1534	1410	1452	1279±32	50.841	13.418	23.400
^{30}Ne	240	1454	1339	1401	1348±17	8.335	0.060	0.012
^{31}Ne	240	1481	1353	1408	1435±22	1.475	4.686	0.001
^{32}Ne	240	1509	1375	1417	1385±33	11.102	0.072	16.463
^{32}Mg	900	1613	1482	1545	1331±24	59.748	17.131	25.437
^{32}Mg	950	1613	1482	1545	1340±24	55.619	15.048	76.418
^{33}Mg	900	1641	1505	1538	1320±23	78.061	25.928	37.001
^{34}Mg	900	1669	1526	1534	1372±46	64.292	17.286	59.202
^{35}Mg	900	1697	1548	1553	1472±70	34.392	3.924	37.198

- [1] F. G. Brickwedde, J. R. Dunning, H. J. Hoge and J. H. Manley, Phys. Rev. **54** 15, (1938).
[2] H. A. Bethe, Phys. Rev. **57** 15, (1940).
[3] F. C. Nix and G. F. Clement, Phys. Rev. **68** 7, (1945).
[4] K. M. Watson, Phys. Rev. **88** 5, (1952).
[5] R. J. Glauber, Phys. Rev. **100** 1, (1955).
[6] C. P. Swann and F. R. Metzger, Phys. Rev. **100** 15, (1955).
[7] W. L. Wong and R. G. Lipes, Phys. Rev. **C 9** 3, (1974).
[8] J. S. Eck, J. R. Leigh, T. R. Ophel and P. D. Clark, Phys. Rev. **C 21** 6, (1980).
[9] H. A. Khan, I. E. Qureshi, W. Westmeier, R. Brandt and P. A. Gottschalk, Phys. Rev **C 32** 5, (1985).
[10] I. Tanihata et al., Phys. Lett. **B 287** 307, (1992).
[11] B. Abu-ibrahim, Y. Ogawa, Y. Suzuki and I. Tanihata, Comp. Phys. Commun **151** 369, (2003).
[12] A. Shukla, B. K. Sharma, R. Chandra, P. Arumugam and S. K. Patra, Phys. Rev. **C 76** 034601, (2007).
[13] S. K. Patra, R. N. Panda, P. Arumugam and Raj K. Gupta, Phys. Rev. **C 80** 064602, (2009).
[14] W. Horiuchi, Y. Suzuki, P. Capel and D. Baye, Phys. Rev. **C 81** 024606, (2010).
[15] K. Minomo et al., Phys. Rev. Lett. 052503, (2012).

- [16] K. Wimmer et al., Phys. Rev. **C** **85** 051603, (2012).
- [17] S. K. Patra and C. R. PraharaJ arXiv: 1002.0654 v1, [Nucl. th] (2010).
- [18] G. Saxena and D. Singh, Int. J. Mod. Phys. **E** **22** 1350025, (2013).
- [19] S. K. Singh, S. Mahapatra and R. N. Mishra, Int. J. Mod. Phys. **E** **22** 1350018, (2013).
- [20] A. Ozawa et al., Phys. Rev. Lett. **84** 24, (2000).
- [21] C. R. Hoffman et al., Phys. Rev. Lett **100** 152502, (2008).
- [22] T. Baumann et al., Nature **449** 1022, (2007).
- [23] A. Ozawa et al., Nucl. Phys. **A** **691** 599, (2001).
- [24] I. Hamamoto, Phys. Rev. **C** **81** 021304(R), (2010); Y. Urata, K. Hagino and H. Sagawa, Phys. Rev. **C** **83** 04130, (2011); K. Minomo, T. Sumi, M. Kimura, K. Ogata, Y. R. Shimizu and M. Yahiro, Phys. Rev. **C** **84** 034602, (2011).
- [25] M. Takechi et al., Phys. Lett. **B** **707** 357-361, (2012).
- [26] E. K. Warburton et al., Phys. Rev. **C** **41** 1147, (1990).
- [27] K. Tanaka et al., Phys. Rev. Lett. **104** 062701, (2010).
- [28] N. Kobayshi et al., arXiv: 1111.7196 v1 [Nucl. ex] (2011).
- [29] I. Tanihata et al., Nucl. Phys. **A** **682** 114c, (2001).
- [30] L. Gaudefray et al., Phys. Rev. Lett **109** 202503, (2012).
- [31] M. Grasso et al., Int. J. Mod. Phys. **E** **18** 2099, (2009); M. Grasso et al., Phys. Rev. **C** **79** 034318, (2009).
- [32] K. T. R. Davies, C. Y. Wong and S. J. Krieger, Phys. Lett. **B** **41** 455, (1972).
- [33] H. A. Wilson, Phys. Rev. **69** 538, (1946).
- [34] X. Campi, D. W. L. Sprung, Phys. Lett. **B** **46** 291, (1973).
- [35] M. Bender, K. Rutz, P. G. Reinhard, J. A. Maruhn, W. Greiner, Phys. Rev. **C** **60** 55, (2003).
- [36] J. Decharge, J. F. Berger, M. Girod, K. Dietrich, Nucl. Phys. **A** **716** 55, (2003).
- [37] A. Shukla, Sven A⁰berg and S. K. Patra, J. Phys. **G: Nucl. Part. Phys.** **38** 095103, (2011).
- [38] S. K. Singh, M. Ikram and S. K. Patra, Int. J. Mod. Phys. **E** **22** 135001, (2013).
- [39] Mahesh K. Sharma and S. K. Patra, Phys. Rev. **C** **87** 044606, (2013).
- [40] B. Behera, X. Viñas, M. Bhuyan, T. R. Routray, B. K. Sharma and S. K. Patra, 2013 J. phys. **G: Nucl. Part. Phys.** (in press); T. R. Routray, X. Viñas, S. K. Tripathy, M. bhuyan, S. K. Patra and B. Behera J. Phys. Conf. Ser. **420** 012114, (2013).
- [41] R. J. Glauber, Phys. Rev. **100** 242, (1955) *ibid*, Lectures on theoretical physics, edited by W. E. Brittin and L. C. Dunham (Int. Sc., New York) **1** 315, (1959).
- [42] P. J. Karol, Phys. Rev. **C** **11** 1203, (1975).
- [43] J. Chauvin et al., Phys. Rev. **C** **28** 1970, (1983).
- [44] Mahesh K. sharma, M. S. Mehta, S. K. Patra, Int. J. Mod. Phys. **E** **22** 135005, (2013).
- [45] G.A. Lalazissis, J. König, and P. Ring, Phys. Rev. **C** **55** 540, (1997).
- [46] J. Boguta and A. R. Bodmer, Nucl. Phys. **A** **292**, 413 (1977).
- [47] W. Pannert, P. Ring, and J. Boguta, Phys. Rev. Lett. **59** 2420, (1987).
- [48] S. K. Patra and C. R. PraharaJ, Phys. Rev. **C** **44** 2552, (1991).
- [49] M. Del Estal, M. Centelles, X. Vinas, and S. K. Patra, Phys. Rev. **C** **63** 024314, (2001).
- [50] P. Ring, Prog. Part. Nucl. Phys. **37** 193, (1996).
- [51] M. Buenerd et al, Nucl. Phys. **A** **424** 313, (1948).
- [52] G. Audi, A. H. Wapstra and C. Thibault, Nucl. Phys. **A** **729** 337, (2003).
- [53] http://amdc.in2p3.fr/masstable/Ame_2011int/mass.
- [54] I. Angeli, K. P. Marinova, Atomic Data and Nuclear Data Table **99** 69-95, (2013).
- [55] National Nuclear Data Center, Brookhven National Laboratory, Based on ENSDF and the Nuclear Wallet Cards.
- [56] W. Horiuchi, Y. Suzuki, B. Abu Ibrahim and A. Kohama, Phys. Rev. **C** **75** 044607, (2007).
- [57] B. Abu-Ibrahim and Y. Suzuki, Phys. Rev **C** **61** 051601, (2000); M. Fukuda et al, Phys. Lett. **B** **208** 339, (1991); A. Ozawa et al., Nucl. Phys. **A** **691** 599, (2001); T. Kobayashi et al., Phys. Lett. **B** **232** 51, (1989); I. Tanihata et al., Phys. Lett. **B** **206** 592, (1988); M. Takachi et al., Nucl. Phys. **A** **834** 412c, (2010).